Analyst

Accepted Manuscript

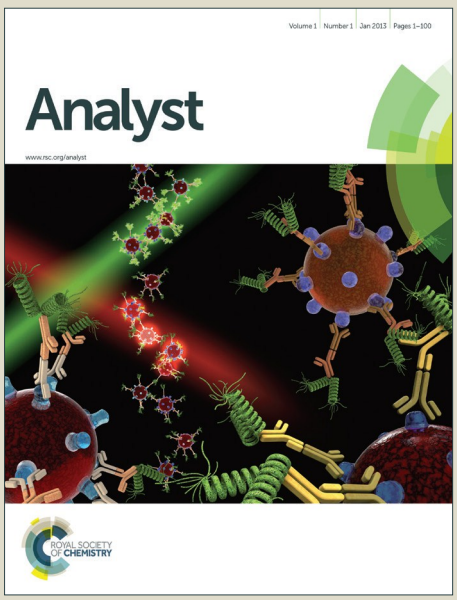

ROYAL SOCIETY OF CHEMISTRY

www.rsc.org/analyst

Journal Name

RSCPublishing

COMMUNICATION

FT-IR imaging for quantitative determination of liver fat content in Non-Alcoholic Fatty Liver

Cite this: DOI: 10.1039/xoxxoooooox

K. Kochan[1,2], E. Maslak[1], S. Chlopicki[1,3] and M. Baranska[1,2,*]

Received ooth January 2012,
Accepted ooth January 2012

DOI: 10.1039/xoxxoooooox

www.rsc.org/

In this work we apply FT-IR imaging of large areas of liver tissue cross-sections samples (~ 5 cm × 5 cm) for quantitative assessment of steatosis in murine model of NAFLD. We quantified the area of liver tissue occupied by lipid droplets (LDs) by FT-IR imaging and Oil Red O (ORO) staining for comparison. Two alternative FT-IR based approaches are presented. The first, straightforward method, was based on average spectra from tissues and provided values of fat content by using a PLS regression model and the reference method. The second one – chemometric-based method – enabled to determine the values of fat content, independently of the reference method by means of *k-means* cluster analysis (KMC). In summary, FT-IR images of large size liver sections may proof useful to quantify liver steatosis without a need of tissue staining.

Introduction

Non-Alcoholic Fatty Liver Disease (NAFLD) is a chronic liver disorder, primarily manifested by an increased accumulation of lipids within the tissue, in the form of lipid droplets (LD's)[1]. In the early stage of NAFLD it is difficult to diagnose this disease due to the lack of both: clear and specific symptoms as well as diagnostic method. Early stage of NAFLD (fatty liver) may progress to Non-Alcoholic Steatohepatitis (NASH) and cirrhosis[2], which finally leads to irreversible liver damage and failure. It is not until the advanced stage of liver damage, affecting the functioning of the whole body, that the symptoms of NAFLD (although still non-specific) become clearly visible. Obviously, diagnosis of the disease at an advanced stage significantly reduces the chances of successful therapy.

The importance of NAFLD relates not only to the fact that it is widespread (WHO estimates that fatty liver affects approximately 30% of the human population of the world)[3] but more importantly, because it represents a manifestation of metabolic syndrome[4] that is associated with diabetes mellitus type II and impose the increased risk of cardiovascular diseases[5]. In fact, association of hepatic steatosis with diabetes and cardiovascular diseases is well established and was reported numerous times[6-7]. The nature of this relationship however, just like the very emergence and development of fatty liver, still remains unclear. NAFLD, often preceding the development of mentioned diseases, is increasingly seen as their common initial state, which can evolve in each of these[8].

The lack of good diagnostic method creates a need in this field, which is not easy to accomplish, since an approach to diagnose early NAFLD would need be sensitive to small changes of biochemical content of the liver.

Fourier Transform Infrared spectroscopy (FT-IR) is a method that possesses huge potential in the field of diagnostics[9-13]. Primarily, it does not require any special sample preparation. Moreover, this technique is adaptable for different types of preparation procedures, including formalin fixed and paraffin embedded specimens, which are known to preserve the structural composition in a good way[10]. Secondly, FT-IR is a sensitive method to obtain information about the biochemical composition of the sample without the use of stains (in the case of which the number of dyes possible to use on the same sample is limited). Moreover, FT-IR is a relatively quick technique of spectroscopic imaging that allows for examination of representative areas of samples. The use of infrared radiation as a source of excitation minimalizes the possibility of a destructive impact of the measurement on the sample.

Infrared imaging has been successfully applied for studies of different tissues and cells, including: liver[10,11], brain[12,13], lungs[14], cervix[15], aorta[16]. As for liver this technique was mostly used to examine cancer[10,11]. IR spectroscopy however is perfectly suited to analyse tissue contents of lipids, as has been

repeatedly proven in various tissues[17-20]. Both, signals in the high wavenumber range (2800 – 3100 cm^{-1}) as well as within the fingerprint region (*f.e.* the band at approximately 1740 cm^{-1}) are well suitable for demonstrating the presence of lipids. In addition, IR spectra allow for a detail investigation of the nature of lipid compounds of the sample, providing for example information on the presence of unsaturated bonds or cholesterol and its esters[15]. The quantitative approach to tissue analysis with the use of FT-IR imaging is, however, not common. Only few examples can be found in the literature[20]. In addition, quantitative determination *via* FT-IR requires supporting results, obtained from other method, as absolute quantification through spectral data itself is not possible[21].

The aim of this work was to develop a methodology for infrared imaging–based quantitative analysis of liver steatosis using a murine model of NAFLD and therefore elaborate new tools applicable for fixed tissue sections.

In the presented work we used a dietary mouse model of Non-Alcoholic Fatty Liver. Fatty liver was induced in C57BL/6J male mice by feeding for 15 weeks with a High Fat Diet, containing 60 kcal % fat (Harlan Laboratories, Germany). For the last 5 weeks of HFD feeding, some mice were subjected to anti-steatotic treatment, so the liver taken from a group of 13 animals had varying degrees of steatosis. After 15 weeks of HFD the mice were euthanized by injection of ketamine (100mg/kg) with xylazine (10mg/kg). The livers were collected immediately after euthanizing the animals and frozen in Optimum Cutting Temperature (OCT) medium in -80°C. Direct preparation of tissue for measurement included cutting them into slices of 10 µm thickness in a cryostat chamber (Leica CM 1950) in -23°C. Tissue sections were subsequently placed on CaF_2 slides and fixed with 4% buffered formalin solution for 10 minutes. The remainders of the fixative were washed out with distilled water (2×5 min).

FT-IR measurements on a macro scale were performed with the use of spectrometer FT-IR Varian 670 equipped with a microscope (15× casseigrain objective) and 128 × 128 MCT Focal Plane Array detector. All spectra were recorded with spectral resolution 8 cm^{-1} in the spectral range from 900 to 3800 cm^{-1} in the transmission mode, by accumulating 64 scans. The imaged areas were approximately ~5×5 cm.

Data analysis was performed with the use of Varian Resolution Pro Software, as well as Cytospec and MatLab. The integration of the band areas was performed in Opus Software. Data preprocessing included: baseline offset correction, normalisation to amide I band (1620 – 1680 cm^{-1}) and quality test (to remove pixels representing the background as well as distorted) performed on the basis of sample thickness criterion in the range 1620 – 1680 cm^{-1}. *K-means* cluster analysis was performed in the range 1420 – 1760 cm^{-1} with the use of 2nd derivatives (calculated with Savitzky-Golay algorithm and 9 smoothing points). The number of classes differed between samples, but typically not exceeded 4.

As a reference method histochemical staining with Oil Red O was used. Oil Red O is a standard diazo dye for lipids and triglycerides. The procedure of staining was done by application of solutions for a certain amount of time, according to following steps: deionized water (3 min.), 60% isopropanol alcohol (2 min.), Oil Red O (30 min.) and deionized water (1 min.). Afterwards the slides with tissues were covered with glycerol gel. The % of tissue covered by lipid droplets was calculated with Columbus Image Data Storage and Analysis System (PerkinElmer, USA) with adapted for Oil Red O stained sections algorithm.

Results and discussion

ORO staining

The first approach to analyse obtained data was a general assessment of the fat content within the liver tissue with the use of a "gold standard" method – histochemical staining with Oil Red O (ORO). Figure 1 presents the results of ORO staining on the basis of which the assessment of the level of steatosis was made: representative stained sections with various content of the fat (Fig.1.A) and results of the determination of the percentage of tissue surface occupied by the lipid droplets (Fig.1.B.)

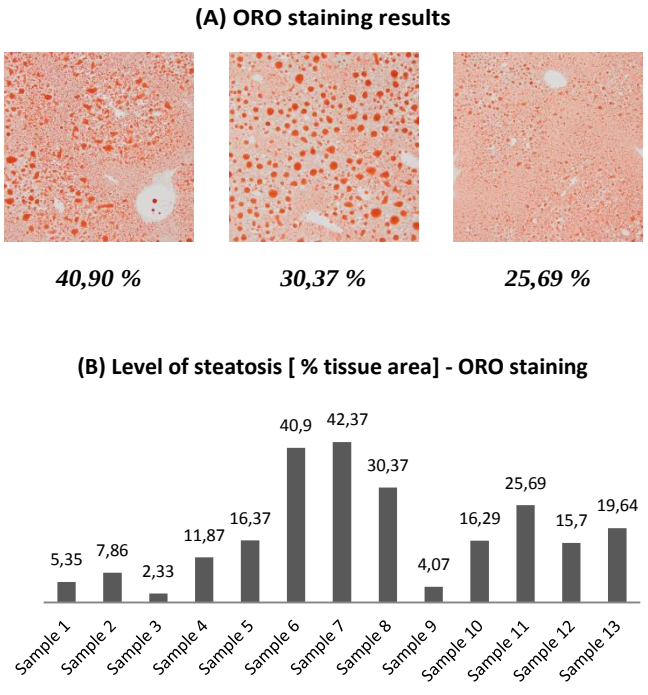

Fig. 1. **(A)** ORO stained sections (magnification 100×) from 3 representative samples with different level of steatosis (with the percentage of fat specified under the photograph) along with **(B)** the level of steatosis expressed as a % of tissue area occupied by lipid droplets. The percentage values (given above each bar and below each photograph) were calculated by Columbus Software.

As can be seen, the degree of fat content was quite different within the studied group (~ 2–42 %), as intended, and thus provided an appropriate series of samples to validate the use of FT-IR for the liver fat content analysis. The ORO staining results reflect well the content of fat within the tissue. On one hand, they allow for a rapid assessment of the overall condition

of the organ, while on the other they enable a more detailed, quantitative research.

FTIR based approaches

Presented approaches involved FT–IR imaging of the whole liver tissue cross-sections. The condition for the correctness of their application is imaging of the whole tissue sections. Even though healthy liver is homogeneous, the pathologically changed liver was featured by heterogeneity and unevenly distributed lipid droplets in different parts of the liver tissue.

Approach 1: A PLS model based on average spectra for each tissue section

The first FT-IR approach is based on obtaining average spectra for each tissue section. After extraction of such spectra, the removal of the baseline and the normalization to the amide I band, two ratios of intensities were calculated: of the high wavenumber range (2800 – 3100 cm^{-1}) to the amide I band and of the area of the band located at 1740 cm^{-1} (C = O stretch vibration[20]) to the amide I band. Ratios calculated in such way, preceded by normalization of all spectra to the amide I band, represent in a straightforward manner the content of lipids within each tissue. Figure 2 presents the calculated ratios from FT-IR averaged spectra from whole tissues.

By comparing the IR–based results from Fig 2.A – B with the ORO assessment it can be seen that the trend of changes between samples is well preserved by both chosen ratios. However, ORO-based approach presents the results in a way, that magnifies the differences between the content of lipids in different tissue sections**.** In the IR-based approach the differences between the extreme samples do not appear to be so big (compare the relation between samples 3 and 6 on Fig.1.B and on Fig. 2A, B). The reason for that is, however, very simple. The appearance of lipid droplets in healthy liver is not excluded entirely, as they can occur in healthy tissues as well, but they are not present in high amounts. Therefore, the percentage of the tissue area occupied by LD's can vary from practically none or very low up to very high. Due to this, in the case of the ORO assessment, the scale of the results varies between 0 – 100. The IR-based approach, on the other hand, involves the use of spectra averaged across the tissue. In such spectrum both chosen signals: the band at 1740 cm^{-1} and the bands in the range 2800 – 3050 cm^{-1} will never be completely absent.

In order to improve the chosen criterion, both ratios (1740 cm^{-1}/amide I and 2800-3050cm^{-1}/amide I) were calculated for healthy liver tissue section, with the use of identical pre-treatment of spectra. The results obtained for the whole sample set were decreased by the value obtained for samples of healthy liver (1740/amide I: 0,07 and 2800-3050/amide I: 0,46). The corrected FT-IR band ratios (Fig.2.C,D) reproduce better the ORO results and can be used to estimate the level of steatosis.

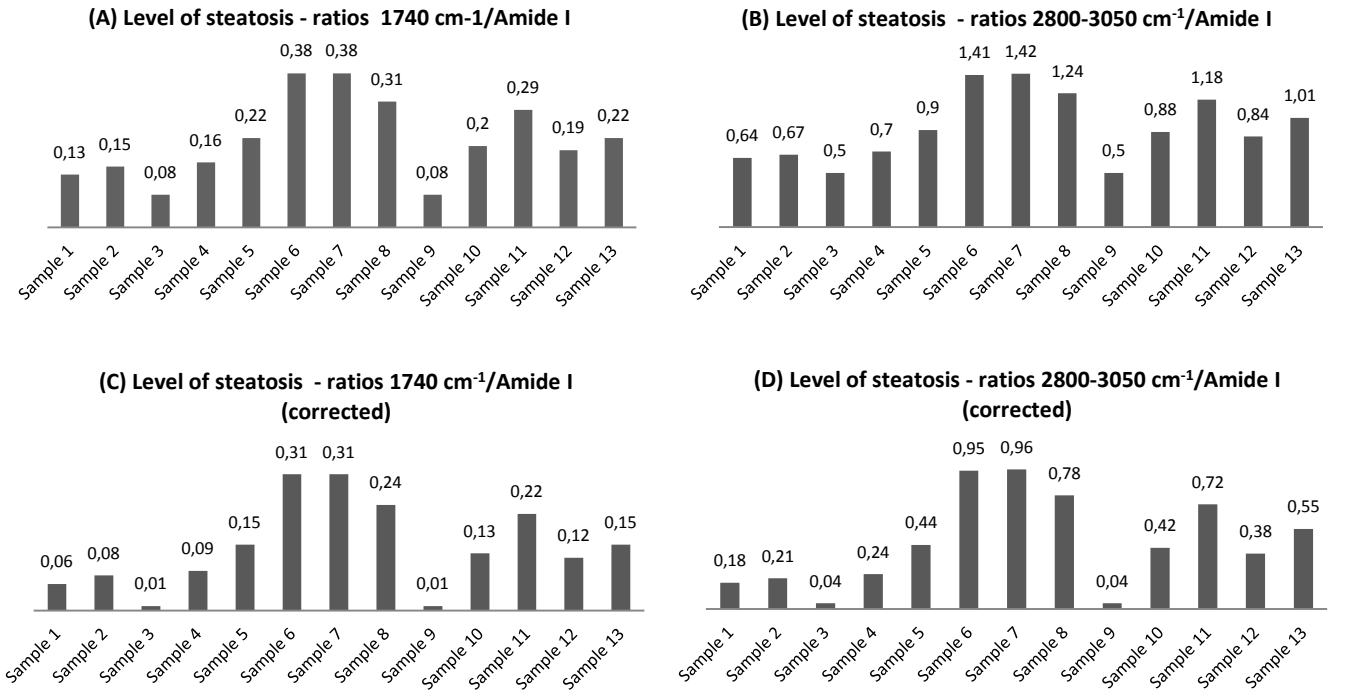

Fig. 2. The values calculated from FT-IR spectra (obtained by averaging the whole tissue measurement), presenting the ratios of chosen bands: **(A)** at 1740 cm^{-1} to the amide I band (1620 – 1680 cm^{-1}) and **(B)** the high wavenumber range (2800 – 3050 cm^{-1}) to the amide I band (1620 – 1680 cm^{-1}). Figures **(C)** and **(D)** represent the same data set, but the values are decreased by the value obtained for the control samples (livers from healthy mice). Presented values were calculated for spectra normalised to the amide I band to reflect more strictly the differences between the level of lipid within the tissue.

For the FT-IR averaged spectra of tissues a PLS regression model for the prediction of the level of steatosis (percentage of the tissue area occupied by LD's) was built. The data set was divided into two: calibration and validation set. Each of them contained samples differing in the level of steatosis. Different pre-treatment procedures and spectral ranges were tested, but eventually the best results were obtained for the model where the pre-treatment of spectra remained the same as for the calculation of ratios and the spectral range of 1580 – 1780 cm^{-1} was included. The parameters of the PLS model (on the basis of calibration set) are presented in Table 1. The results of prediction performed with the use of it on the validation model are presented on Fig. 3 (and Table S1, supplementary information).

Table 1. Parameters of the PLS regression model.

Parameter	Value	Parameter	Value
Slope	0,9805945	R-Square	0,9805948
Offset	0,363441	RMSEC	2.0094995
Correlation	0,9902497	SEC	2.1482458
R2 (Pearson)	0,9805945	Bias	-4.7684×10^{-7}

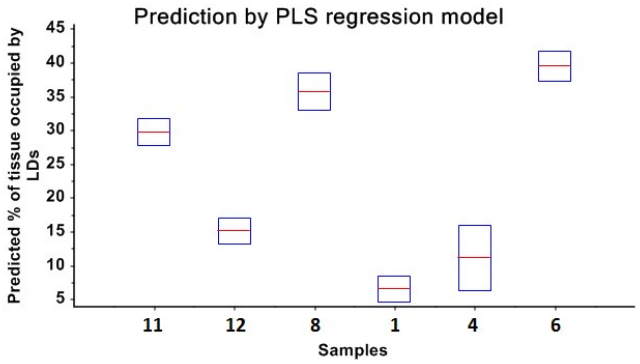

Fig. 3.Results of prediction of the percentage of tissue occupied by LD's performed with the use of build PLS model for the validation set (value – red line, standard deviation – blue squares). PLS model is based on FT-IR spectra averaged for whole tissue sections, in the range 1580 – 1780 cm^{-1}.

The model allowed for a successful prediction of the percentage of tissue covered by lipid droplets, although the standard deviation appears to be higher for tissues with medium developed steatosis. Nonetheless, the predicted values remain in good agreement with the ORO – based results (see Table 2, summarising the FT-IR based approaches).

Approach 2: The ratio of pixels assigned to the lipid class to all pixels

The second possible FT-IR approached involved the use of entire spectral images, obtained for large areas of tissue sections. By performing cluster analysis (*k-means*) on the obtained FT-IR images it is possible to separate a class of clearly higher lipid content. Subsequently, analogously to the ORO-based approach, by calculating the ratio of pixels assigned to the lipid class to all pixels representing the tissue it is possible to determine the percentage of tissue occupied by LDs. An example of this approach is presented on Fig. 4.

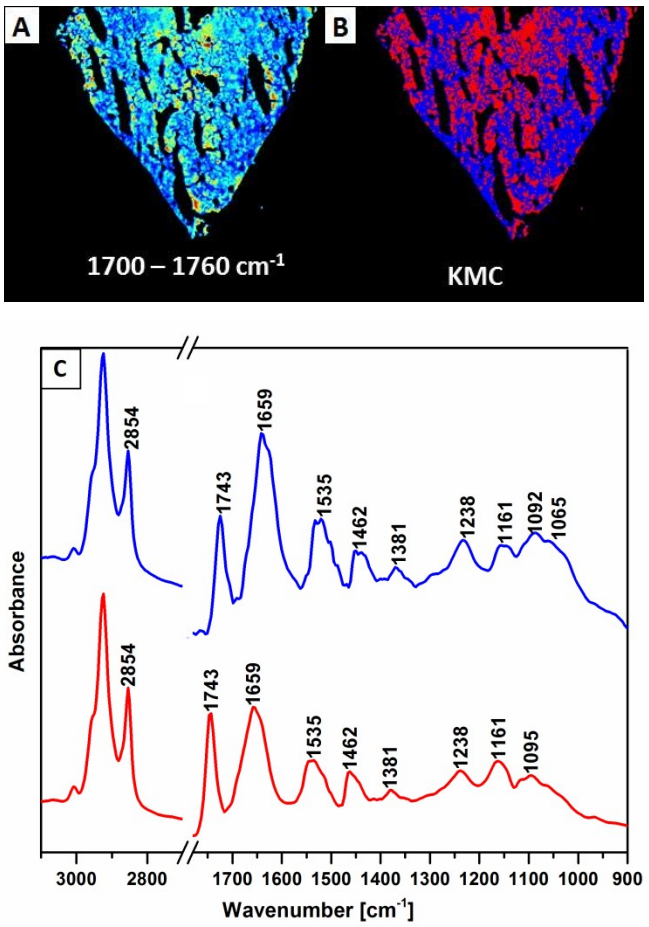

Fig. 4. An example of FT-IR results of large tissue section analysis: **(A)** integration of the C=O stretching band (in the range 1700 – 1760 cm^{-1}) along with the KMC results: **(B)** distribution of lipid class (red) and **(C)** corresponding KMC averaged spectra of classes with assigned most intense bands.

This approach, however, is associated with a certain error, especially in the case of microvesicular steatosis or any early stage of LD's development. This results from the droplets size and shape. In cases of an early development or manifestation in the form of microvesicular steatosis, the droplets size tend to be below the spatial resolution of pixels in FT-IR images (~ 5×5 μm^2). Thus, the assessed value will be overestimated (when the droplet is smaller than the pixel but takes more than 50% of its area) or underestimated (if the droplet covers less than 50% of pixels area). This problem applies also to a more advanced stage, when single LD's occupy an area of several pixels. Due to their round shape, droplets will never fit perfectly into the image constructed from square pixels. Moreover, the cluster analysis approach does not allow (in the case of attempts to develop a universal model) for a clear definition of when a class can be classified as a tissue and when as a LD. This is due to the fact that the lipid content (and therefore – spectrum) within the tissue

(excluding lipid droplets) is different for the tissues with advanced steatosis and without it (or on early stage of development). In general, spectra of the "non-lipid" classes from livers with advanced steatosis present much more intense lipidic signals compared to "non-lipid" classes from healthy livers. Therefore, a clear criterion for the division between the lipid and non-lipid classes (*f.e.* a particular value of lipid/protein ratio) that would be applicable for all tissues, regardless of the level of steatosis development cannot be defined. Each tissue should be rather considered individually.

Despite potential sources of errors described above, with a careful approach, it is possible to obtain the percentage values of tissue occupied by LD's. These results still remain in good correlation with the values obtained by ORO-based approach (Fig.5 and Table 2). Therefore, this approach – like the previous, based on average spectra – also appears to be suitable for assessment of the degree of steatosis development.

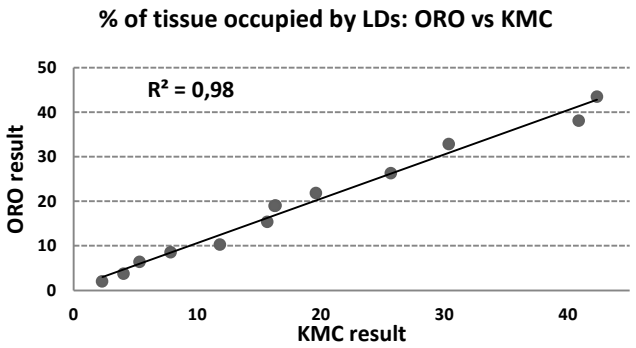

Fig. 5. Correlation between the percentage value of tissue occupied by LD's obtained by ORO-based and KMC-based approach. Results from individual samples are given in Table 2.

Table 2. Results of the assessment of % of tissue occupied by LD's obtained with all presented approaches: from ORO staining and from FT-IR spectra: PLS-based and KMC-based analyses. The SD values for the PLS-based approach are presented in Table S1 (supplementary information).

Sample	% of tissue occupied by LDs		
	PLS	KMC	ORO
Sample 1	6,49	6,33	5,35
Sample 2	11,45	8,52	7,86
Sample 3	1,04	1,97	2,33
Sample 4	11,09	10,24	11,87
Sample 5	18,67	18,96	16,37
Sample 6	39,47	38,05	40,9
Sample 7	41,05	43,38	42,37
Sample 8	35,70	32,8	30,37
Sample 9	1,04	3,66	4,07
Sample 10	17,10	18,93	16,29
Sample 11	29,71	26,2	25,69
Sample 12	15,14	15,29	15,7
Sample 13	19,46	21,81	19,64

Conclusions

FT-IR imaging is a technique with huge potential in the field of the study of biological materials. The simplicity of sample preparation and the complexity of the obtained results makes it a tool of choice for tissue studies. Additionally, it provides a possibility not only to examine bigger groups of samples but also to investigate large areas, thereby eliminating both: the impact of individual variability and randomness of the selection of investigated area. In the presented work we applied FT-IR imaging of large pieces of liver cross-sections for quantitative determination of the steatosis that was performed on the basis of percentage of liver tissue occupied by lipid droplets. We presented two approaches: the first, based on the averaged spectra of a tissue and second, based on the KMC analysis of each imaged specimen. Both approaches enabled to obtain results, which remain in a very good correlation with ORO results and therefore allowed to achieve the same objective as ORO staining. In the case of spectroscopic methods, however, the obtained experimental data can be additionally analysed in terms of liver contents of other components. In the first approach presented in this work, a simple calculation of the ratio of lipid to protein bands (preceded by normalisation to amide I band) provided a straightforward manner to quantify liver lipid content. By the use of PLS regression model and results obtained with ORO staining it was possible to obtain explicit values. The second approach proposed in this work allowed, in an analogous way to the ORO-based method, to assess the percentage of tissue affected by pathological steatotic changes. It is worth to add, that the first approach did not require the use of any advanced chemometric methods and was easier to implement in terms of analysis. However, it did not allow to determinate the absolute value of fat liver content without the aid of another technique. The second approach, in turn, required a more time-consuming analysis, but it enabled to determine absolute value of fat content without a need of a reference method. Altogether, FT–IR imaging of large areas of liver cross-section seem to represent a powerful and reliable method for the quantitative assessment of liver steatosis, that may prove useful to assess liver disease progression in animal models of NAFLD as well as in patients.

Acknowledgements

This work was supported by the European Union under the European Regional Development Fund (grant coordinated by JCET-UJ, POIG.01.01.02-00-069/09) and National Science Center (grant DEC-2013/09/N/NZ7/00626).

Notes and references

[1]*Jagiellonian Centre for Experimental Therapeutics (JCET), Jagiellonian University, Krakow, Poland,*

[2]*Faculty of Chemistry, Jagiellonian University, Krakow, Poland.*

[3]*Department of Experimental Pharmacology, Jagiellonian University Medical College, Krakow, Poland*

**email:baranska@chemia.uj.edu.pl*

1 R. Lomonaco, N.E. Sunny, F. Bril and K. Cusi., *Drugs*, 2013, **73(1):**1-14.
2 N. Bhala, P.Angulo, D. van der Poorten, E. Lee, J.M. Hui, G. Saracco, L.A. Adams, P. Charatcharoenwitthaya, J.H. Topping, E. Bugianesi, C.P. Day, J. George, *Hepatology*, 2011, **54(4)**:1208-16.
3 World Health Organisation, WHO: www.who.int.
4 E. Vanni, E. Bugianesi, A. Kotronen, S. De Minicis, H. Yki-Järvinen, G. Svegliati-Baroni, *Dig Liver Dis.*, 2010, **42(5):**320-30.
5 P.L. Huang, *Dis Model Mech*., 2009, **2(5-6):**231-7.
6 K. H. Williams, N. A. Shackel, M. D. Gorrell, S. V. McLennan, S. M. Twigg, *Endocrine Reviews*, 2013, **34(1):**84-129
7 M. Gaggini, M. Morelli, E. Buzzigoli, R.A. DeFronzo E. Bugianesi, A. Gastaldelli, *Nutrients*, 2013, **10;5(5)**:1544-60.
8 Q.M. Anstee, G. Targher, C.P. Day,*Nat Rev Gastroenterol Hepatol.*, 2013, **10(6)**:330-44.
9 K. Das, C. Kendall, M. Isabelle, C. Fowler, J. Christie-Brown, N.Stone, *J Photochem Photobiol B.*, 2008,**18**;92(3):160-4.
10 K. Kochan, P. Heraud, M. Kiupele, V. Yuzbasiyan-Gurkan, D. McNaughton, M. Baranska, B.R. Wood, *Analyst*, 2015, DOI: 10.1039/C4AN01901F
11 K. Thumanu, S. Sangrajrang, T. Khuhaprema, A. Kalalak, W. Tanthanuch, S. Pongpiachan, P. Heraud, *J Biophotonics.*, 2014,**7(3-4)**:222-31.
12 M.J. Hackett, J. Lee, F. El-Assaad, J.A. McQuillan, E.A. Carter, G.E. Grau, N.H. Hunt, P.A. Lay, *ACS Chem Neurosci.*, 2012,**19;3(12):**1017-24.
13 N. Bergner, B. F. M. Romeike, R. Reichart, R. Kalff, C. Krafft, J. Popp, *Clinical and Biomedical Spectroscopy and Imaging II*, N. Ramanujam and J. Popp, eds., Vol. 8087 of Proceedings of SPIE-OSA Biomedical Optics (Optical Society of America, 2011), paper 80870X.
14 P. D Lewis**,** K. E. Lewis**,** R.Ghosal**,** S.Bayliss**,** A. J. Lloyd**,** J. Wills**,** R. Godfrey**,** P.Kloer**,** L. A. J. Mur**,** *BMC Cancer*, 2010, **10**:640, DOI:10.1186/1471-2407-10-640.
15 B.R. Wood,, L. Chiriboga,H. Yee,M.A. Quinn, D. McNaughton, M. Diem, *Gynecol Oncol.*, 2004,**93(1)**: 59–68.
16 K. M. Marzec, T. P. Wrobel, A. Ryguła, E. Maślak, A. Jasztal, A. Fedorowicz, S. Chlopicki, M. Baranska, *J. of Biophot.*, 2014, **7(9)**: 744–756.
17 F. Kucuk Baloglu, S. Garip, S. Heise, G. Brockmann, F. Severcan, *Analyst*, 2015, **140 (7)**: 2205-2214.
18 M.J. Baker, J.Trevisan, P. Bassan, R. Bhargava, H.J. Butler, K.M. Dorling, P.R. Fielden, S.W. Fogarty, N.J. Fullwood, K.A. Heys, C. Hughes, P. Lasch, P.L. Martin-Hirsch, B. Obinaju, G.D. Sockalingum, J. Sulé-Suso, R.J. Strong, M.J. Walsh, B.R. Wood, P. Gardner, F.L. Martin, *Nat Protoc*., 2014, **9(8)**:1771-91.
19 S.G. Kazarian, K.L.A. Chan, *Biochimica et Biophysica Acta (BBA) - Biomembranes*, 2006, Vol. 1758, Iss. 7, p.858-867.
20 I. Dreissig, S. Machill, R. Salzer, C. Krafft, *Spectrochimica Acta Part A: Molecular and BiomolecularSpectroscopy*, 2009;**71(5)**:2069–2075.
21 K.M. Gough, D. Zelinski, R. Wiens, M. Rak, I.M.C. Dixon, *Analytical Biochemistry*, 2003, **316** : 232–242.